Supporting Information

pH-Responsive iron-loaded carbonaceous nanoparticles with chemodynamic therapy based on Fenton reaction

Nianlu Li [a,c,1] Gaorui Zhang [b,d,1], Jinhua Zhan [a,*], Dexin Yu [b,d,*]

a School of Chemistry and Chemical Engineering, Shandong University, Jinan, 250100, China

b Department of Radiology, Qilu Hospital of Shandong University, Jinan, Shandong, 250012, China

c Physical and Chemical Laboratory, Shandong Academy of Occupational Health and Occupational Medicine, Shandong First Medical University & Shandong Academy of Medical Sciences, Jinan, 250000, China

d Translational Medicine Research Center in Nano Molecular and Functional Imaging of Shandong University, Jinan, 250100, China

* Corresponding author.

E-mail addresses: jhzhan@sdu.edu.cn (Jinhua Zhan), yudexin0330@sina.com (Dexin. Yu)

[1] These authors contributed equally to this work.

Experiment section

The determination of Fe loading on CNPs

To determine the Fe loading on CNPs, ICP-MS was used to test the mount of Fe. First, a certain amount of dried CNPs were dispersed in 50 mL water under ultrasonication and a series of $FeCl_2 \bullet 4H_2O$ were added. Then the final solutions were ultrasonicated for another 0.5 h and stirred for 12 h at room temperature. Finally, the obtained products of CNPs@Fe were washed with ethanol and water. The samples were acquired after dried and digested with nitric acid. The resulted solutions were collected for ICP-MS testing.

The determination of CNPs number

To determine the number of CNPs, fluorescein labeling is required. fluorescein-CNPs were prepared using the fluorescein isothiocyanate hydroxyl labeling method [1]. Briefly stated as follows: CNPs (0.1 g) were dissolved in dimethylsulfoxide (4 mL) under ultrasonic and then pyridine (5 μL) and fluorescein isothiocyanate isomer I (FITC) were added. Subsequently, dibutyltin dilaurate (2 μL) was added and the solution was placed at 95 °C for 2 h. The obtained results were centrifuged and washed. Finally, the precipitate was re-dispersed in water for dialysis to remove FITC. The final product was tested by flow cytometry.

Preparation of Fe_3O_4

L-Arginine (3.0 g) and $FeCl_3 \bullet 6H_2O$ (0.5 g) were added to a component solvent containing water (10 mL) and glycerol (10 mL) under stirring. The solution was transferred into a 50 mL Teflonlined stainless steel autoclave and heated to 200 ºC for 6 h. After the autoclave cooled to room temperature, the product was separated from the suspension by magnetic force and washed with water. Finally, the product was dried [2].

Reference

[1] A.N. Belder DE, K. Granath. Preparation and properties of fluorescein-labelled dextrans. Carbohydrate Research. 30(2) (1973) 375-378.

[2] Y. Lai, W. Yin, J. Liu, R. Xi, J.Zhan. One-Pot Green Synthesis and Bioapplication of L-Arginine Capped Superparamagnetic Fe_3O_4 Nanoparticles Nanoscale Res Lett 5 (2010) 302–307.

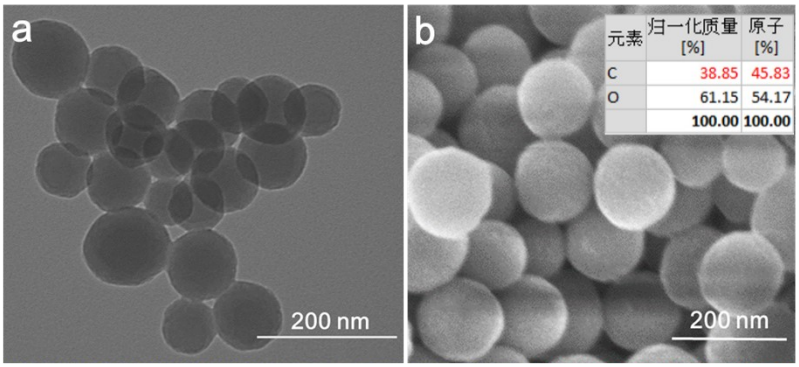

元素	归一化质量 [%]	原子 [%]
C	38.85	45.83
O	61.15	54.17
	100.00	100.00

Fig. S1. (a) TEM of CNPs; (b) SEM of CNPs (insert is the content of C/O).

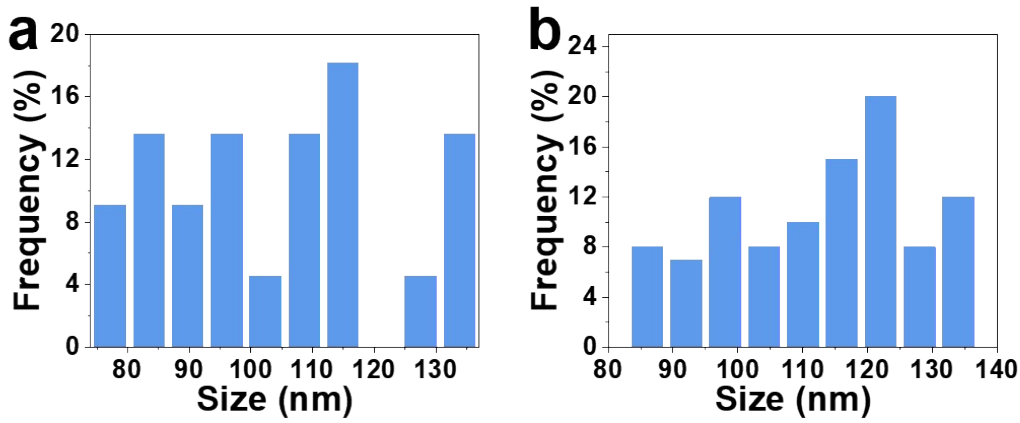

Fig. S2. Size distribution of CNPs@Fe calculated from Figs. 1a and 1b, respectively.

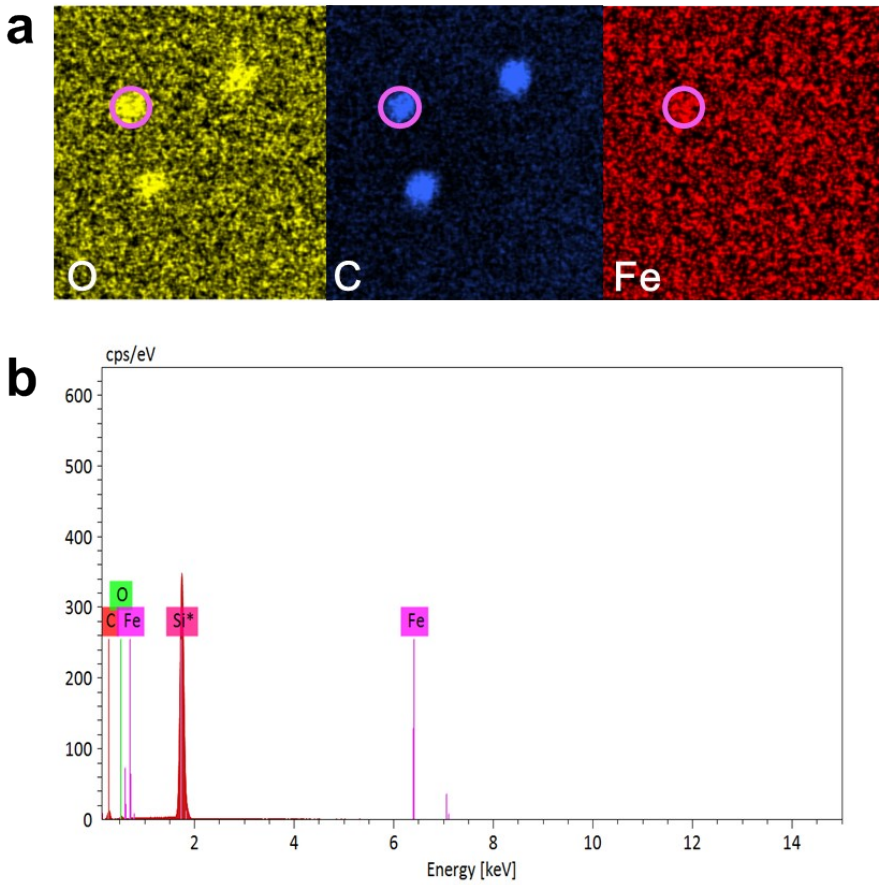

Fig. S3. (a) EDX elemental mapping of O, C, and Fe; (b) EDX spectroscopy of O, C, and Fe.

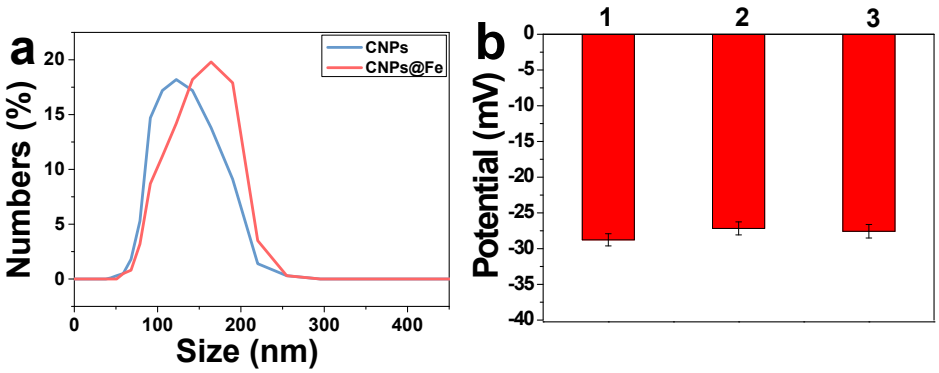

Fig. S4. (a) Hydrodynamic diameter distributions of CNPs and CNPs@Fe; (b) ζ potential of (1) CNPs and (2) CNPs@Fe in HAc-NaAc (pH = 7.4), (3) ζ potential of CNPs@Fe treated in HAc-NaAc (pH = 7.4) for 12 h.

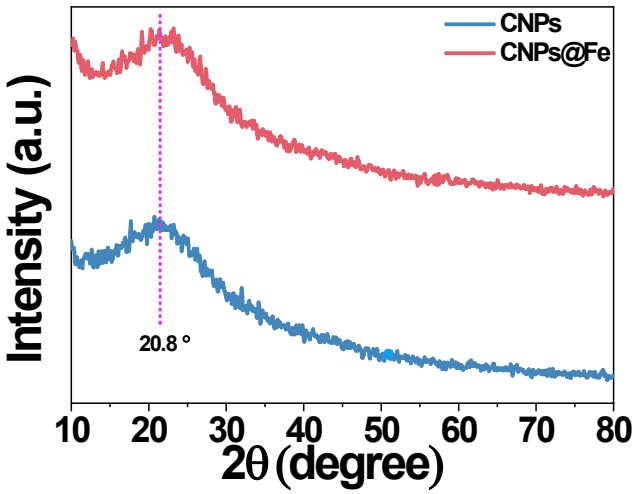

Fig. S5. XRD pattern of CNPs and CNPs@Fe.

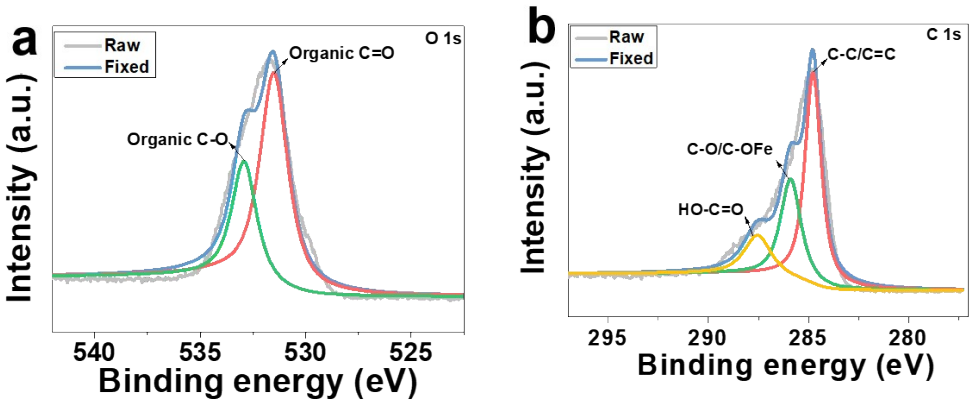

Fig. S6. XPS spectra of (a) O 1s and (b) C 1s.

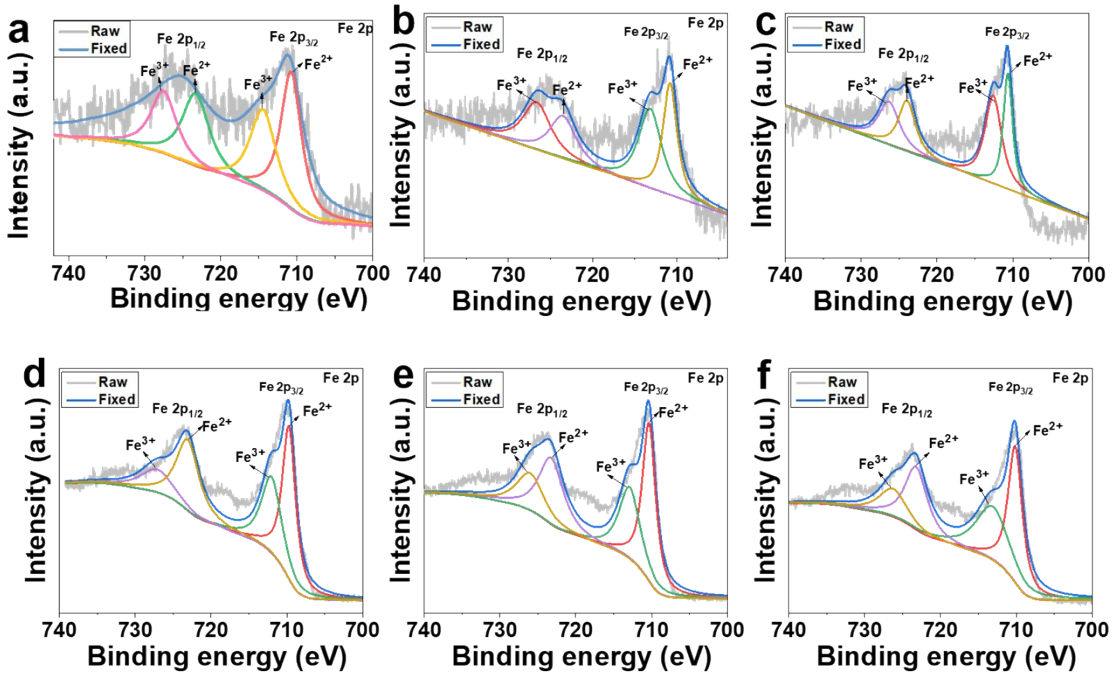

Fig. S7. XPS spectra of Fe 2p in CNPs@Fe (a) before used, (b) treated in pH 6.0, (c) treated in pH 5.0; XPS spectra of Fe 2p in Fe_3O_4 (d) before used, (e) treated in pH 6.0, (f) treated in pH 5.0.

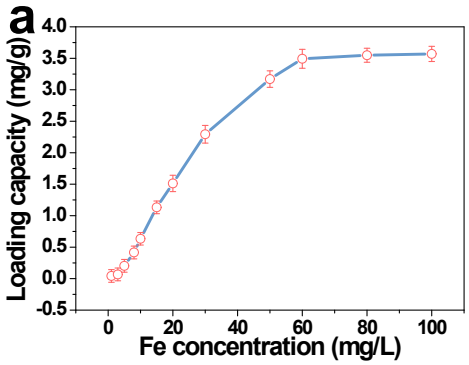

Fig. S8. (a) Fe loading capacity of CNPs at various concentrations of Fe^{2+}; (b) Time dependent release of Fe from CNPs@Fe at different pH values.

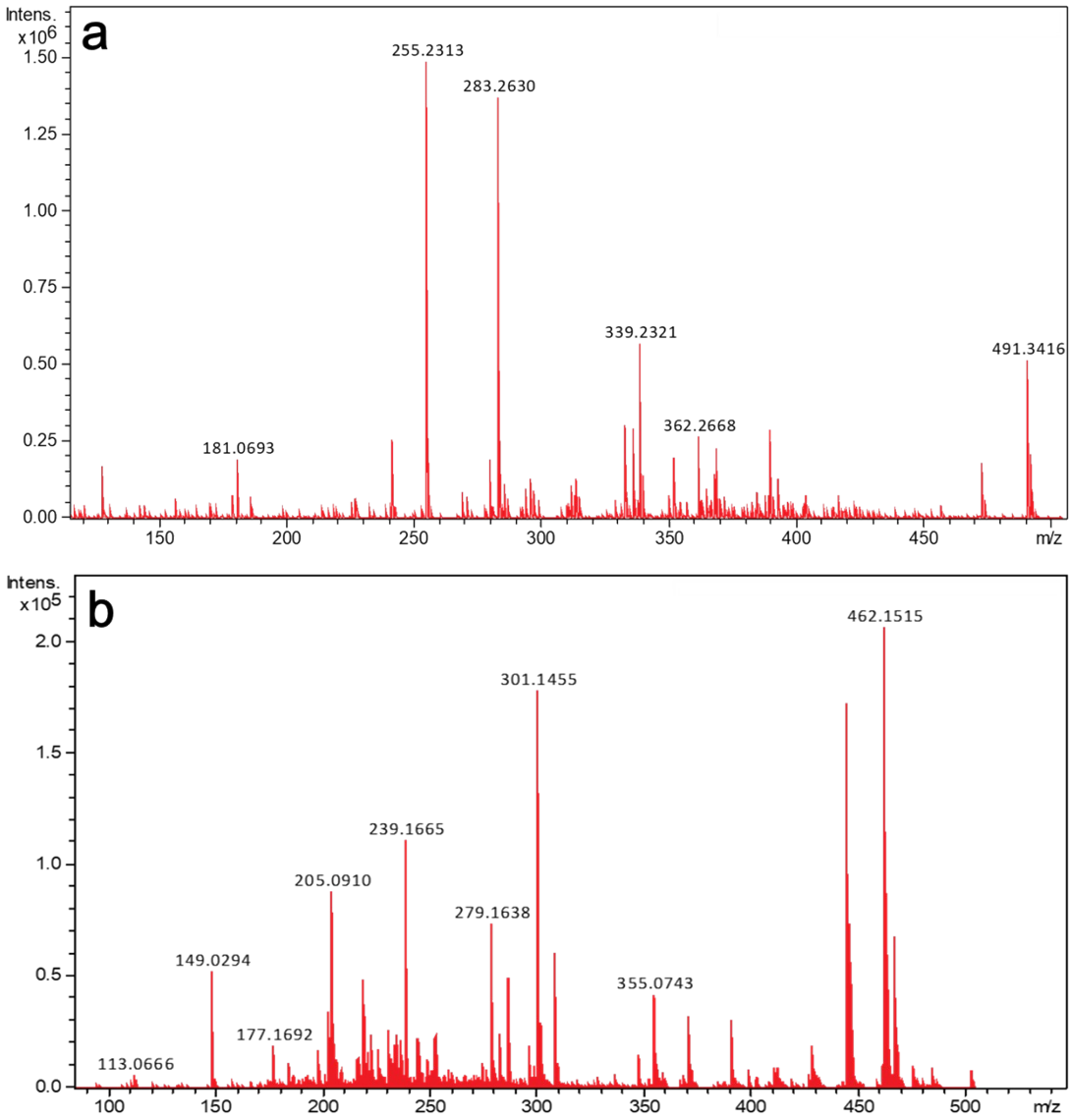

Fig. S9. Mass spectra of CNPs in the (a) negative ion mode and (b) positive ion mode using a direct infusion into a DART-TOF-MS instrument.

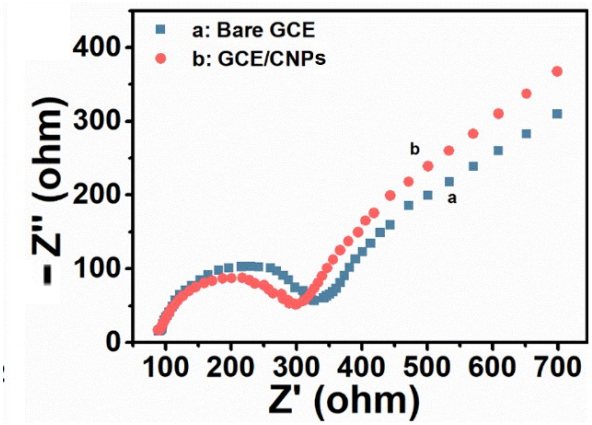

Fig. S10. Electrochemical impedance spectroscopy of the different electrodes in in 0.1 mol/L KCl containing 5 mmol/L $[Fe(CN)_6]^{3-/4-}$. The frequency range is between 0.01 and 100,000 Hz with amplitude of 5 mV.

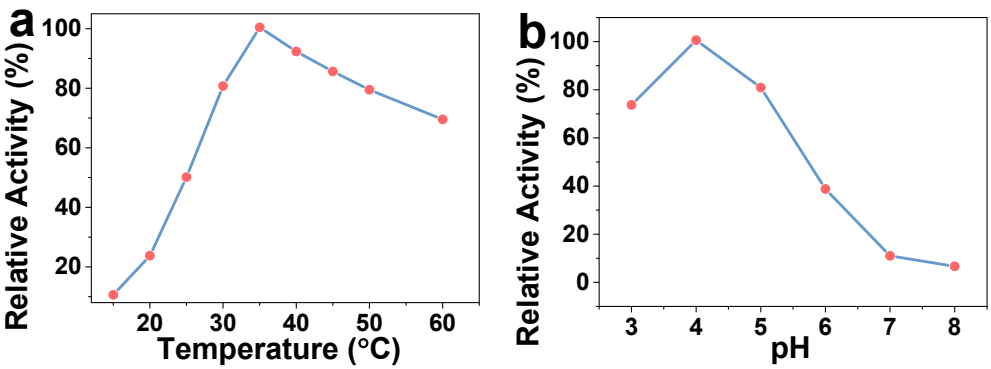

Fig. S11. Effects of (a) temperature at pH 4.0 and (b) pH at a temperature of 35 °C on catalytic activity of CNPs@Fe.

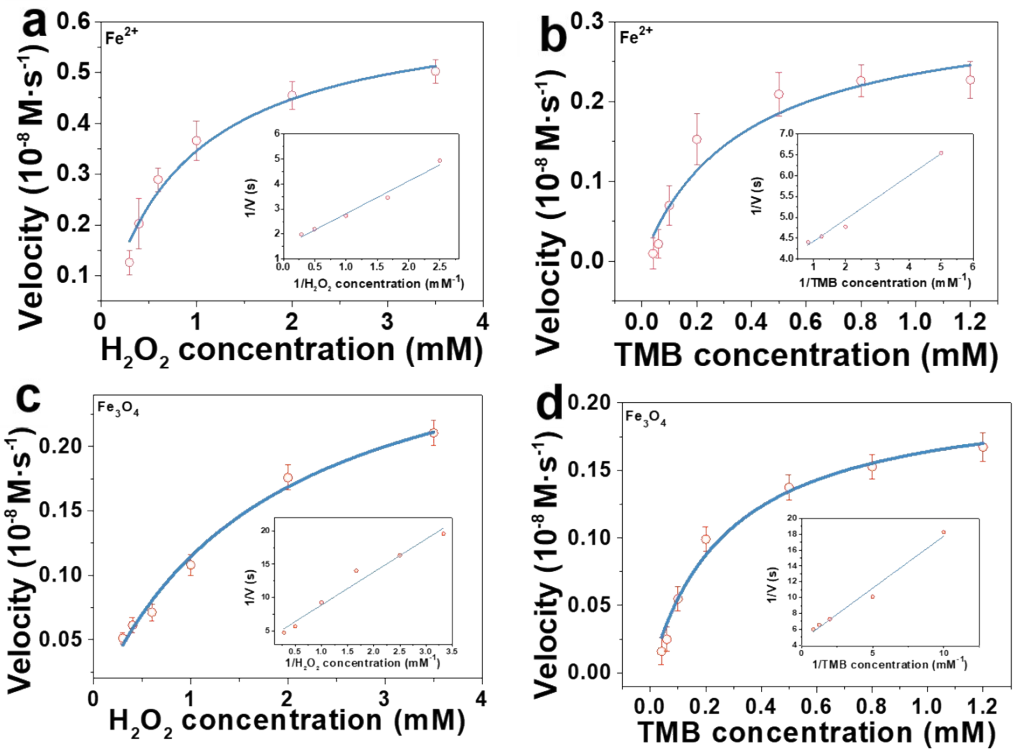

Fig. S12. Steady-state kinetic assay using H_2O_2 and TMB as substrates, respectively. (Insert: Double-reciprocal plots). Conditions: 180 ppm of Fe^{2+} (a and b), 2.0 ppm of Fe_3O_4 (c and d), HAc-NaAc buffer (0.01 M, pH 5.0), 35 ºC.

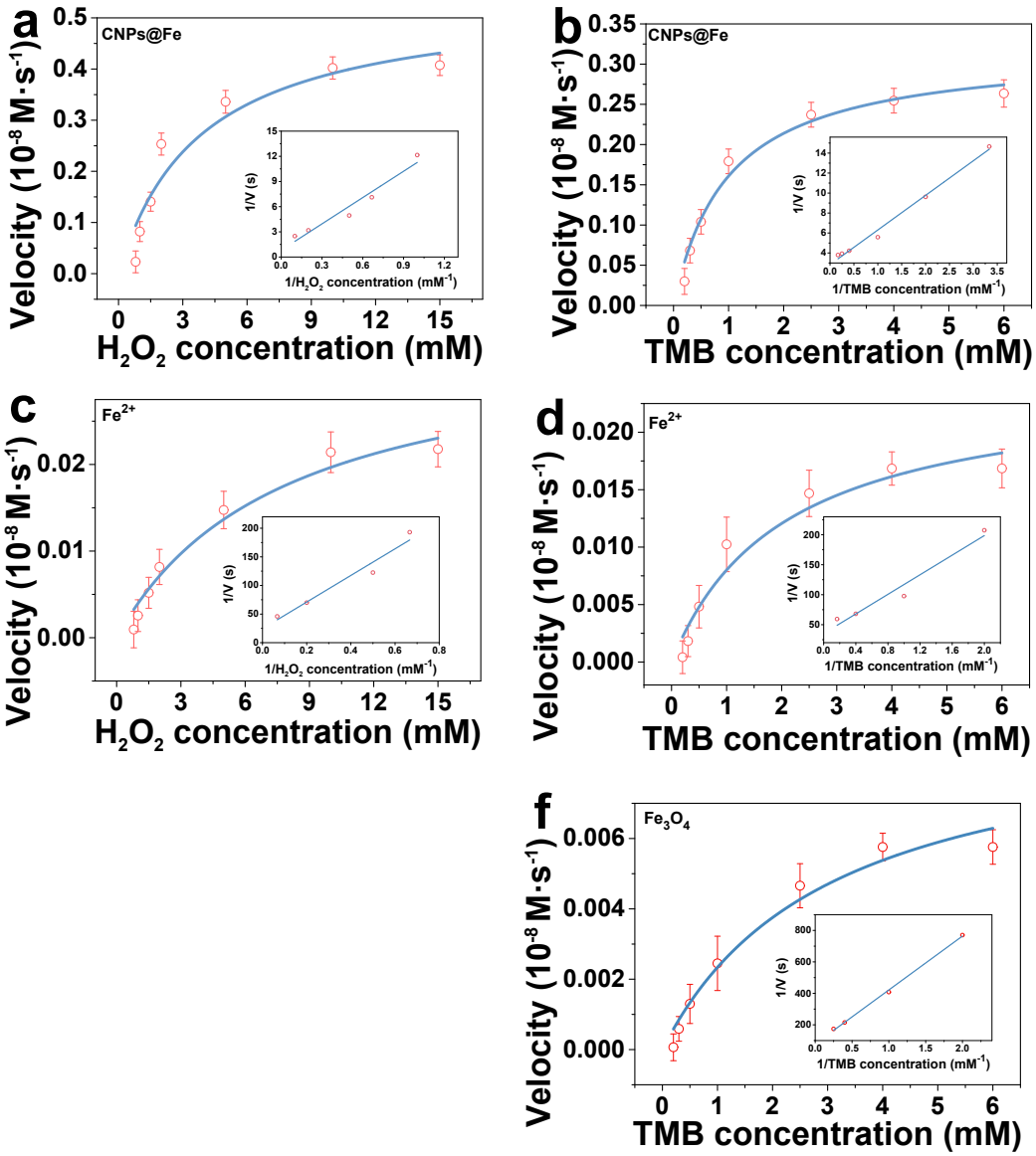

Fig. S13. Steady-state kinetic assay using H_2O_2 and TMB as substrates, respectively. (Insert: Double-reciprocal plots). Conditions: 50 μg/mL of CNPs@Fe (a and b), 180 ppm of Fe^{2+} (c and d), 2.0 ppm of Fe_3O_4 (e and f). HAc-NaAc buffer (0.01 M, pH 6.0), 35 ºC.

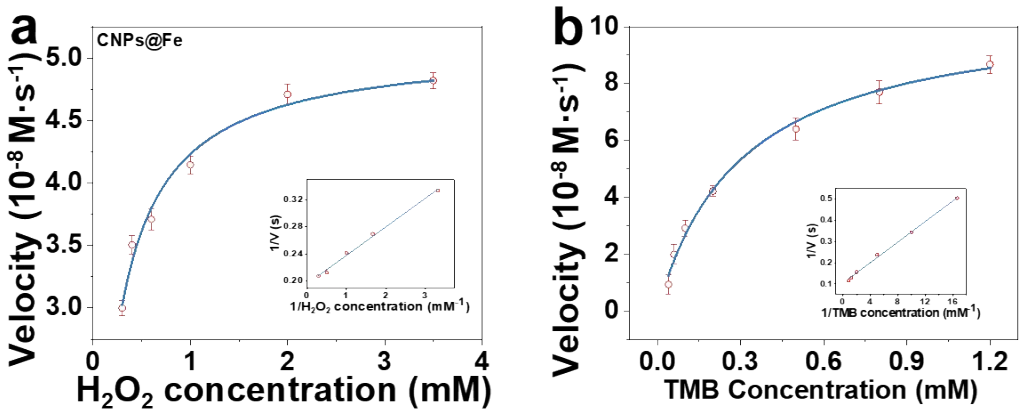

Fig. S14. Steady-state kinetic assay of CNPs@Fe (50 μg/mL) in HAc-NaAc buffer (0.01 M, pH 4.0) using (c) H_2O_2 and (d) TMB as substrates, respectively. (Insert: Double-reciprocal plots).

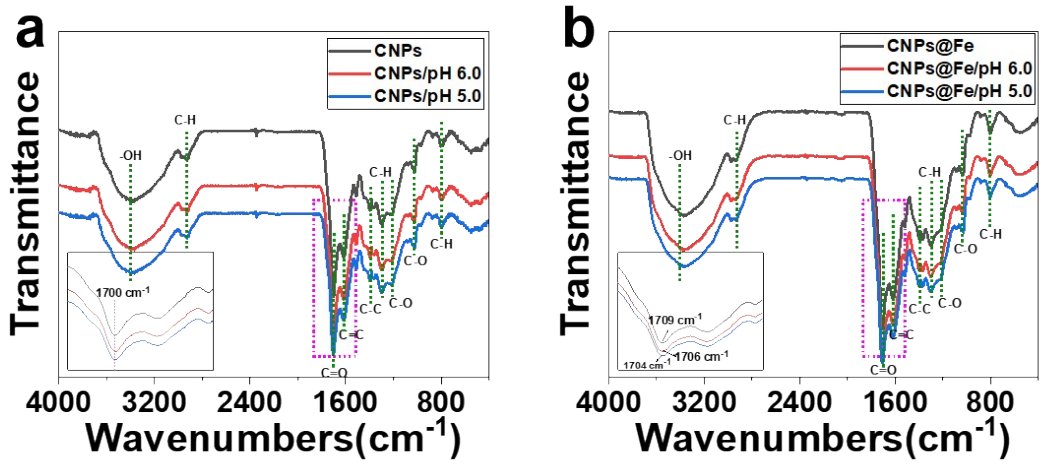

Fig. S15. FTIR spectra of (a) CNPs and (b) CNPs@Fe treated in different systems.

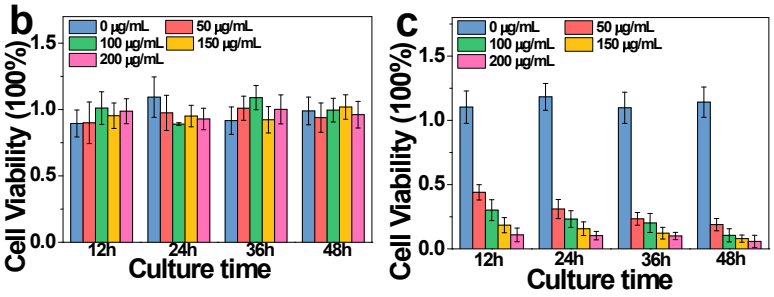

Fig. S16. (a) Effects of the concentrations of CNPs on PANC-02 cells viability at different time intervals. (b) Effects of the concentration of CNPs@Fe on hTERT-HPNE cells viability at different time intervals. (c) Effects of the concentrations CNPs@Fe on PANC-02 cells viability at different time intervals.

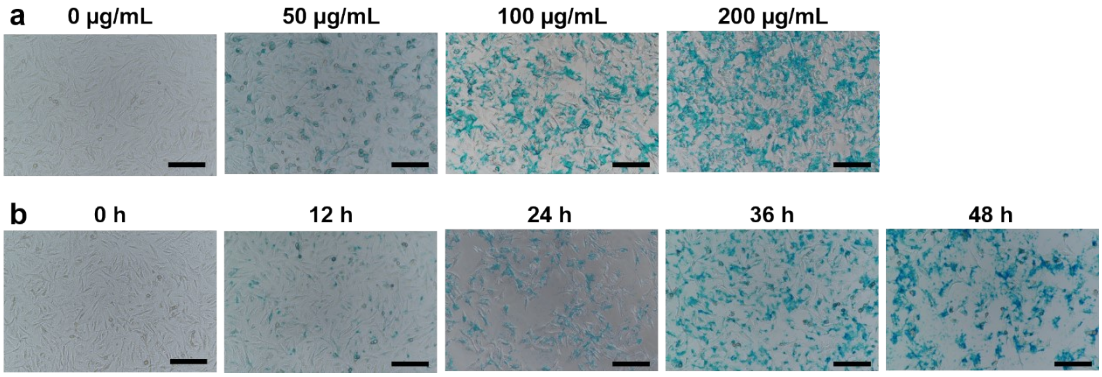

Fig. S17. Prussian blue staining of 4T1 cells after incubation (a) with different concentrations of CNPs@Fe and (b) for different time.

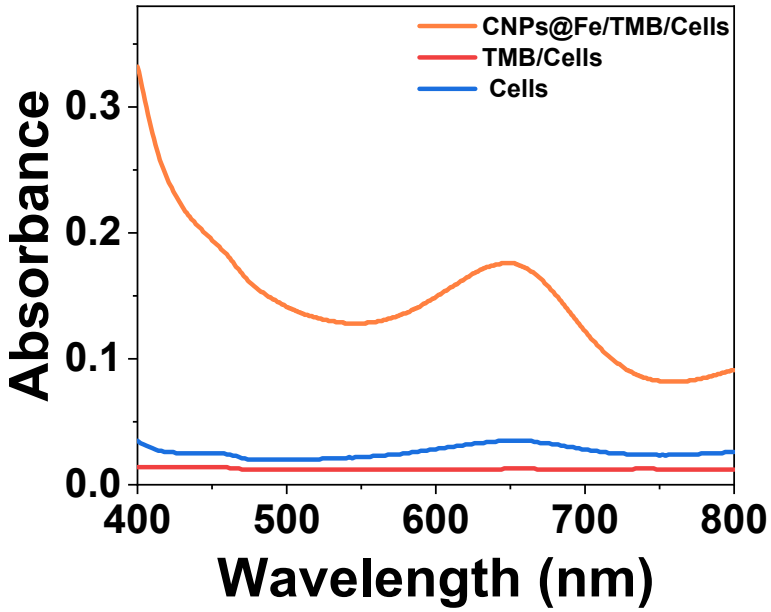

Fig. S18. The UV-vis absorption spectra of different systems.

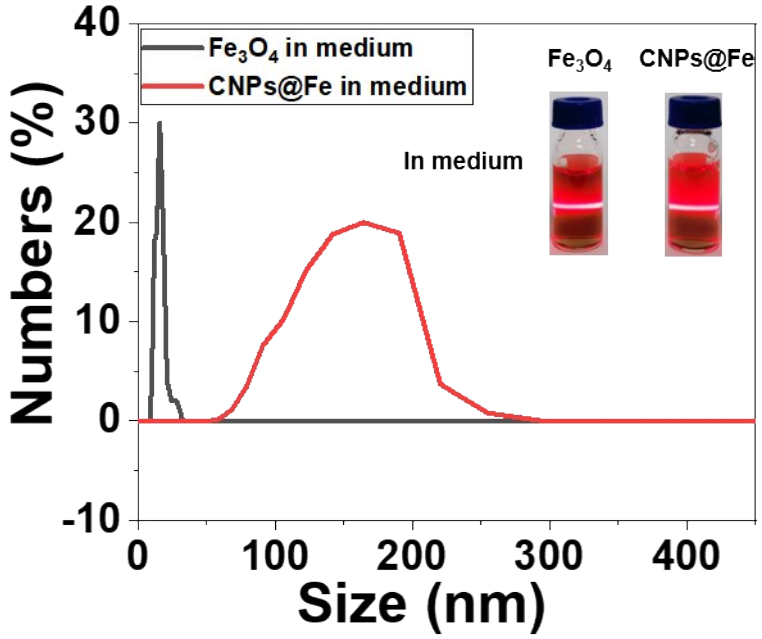

Fig. S19. Hydrodynamic diameter distributions of Fe_3O4 and CNPs@Fe (insert is the Tyndall effect of Fe_3O_4 and CNPs@Fe).

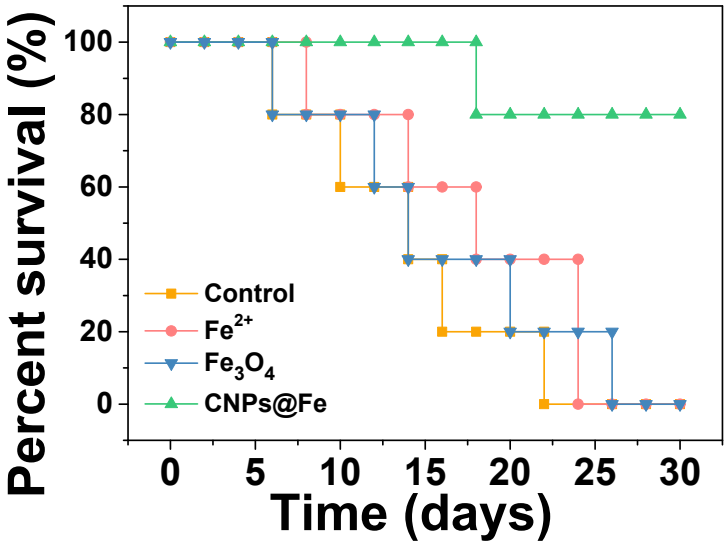

Fig. S20. Survival curves of 4T1 tumor-bearing mice in different groups.

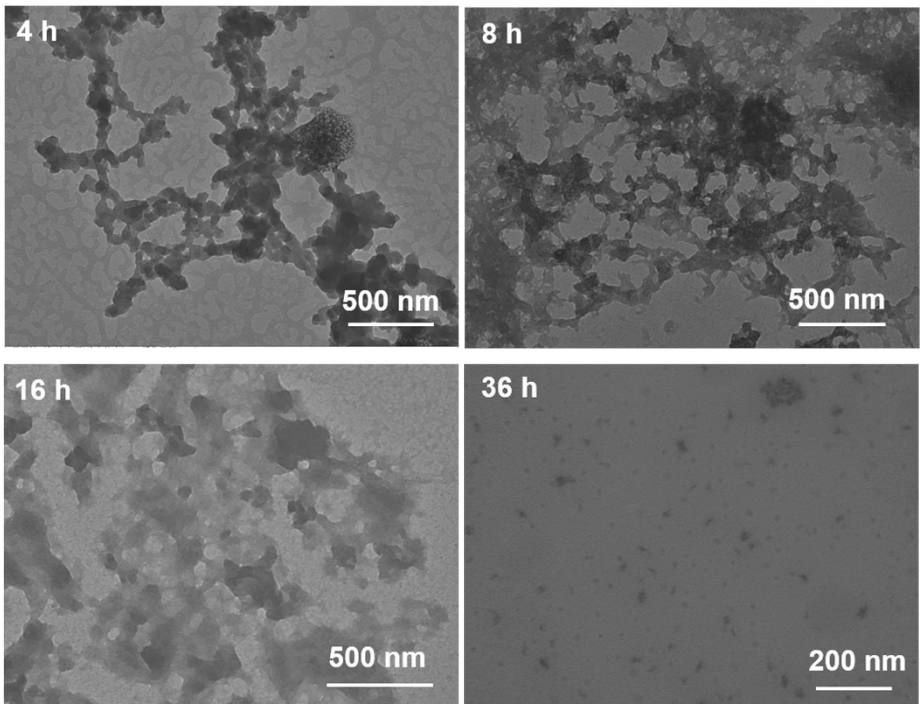

Fig. S21 Time-dependent TEM images of CNPs@Fe after being soaked into enzyme.

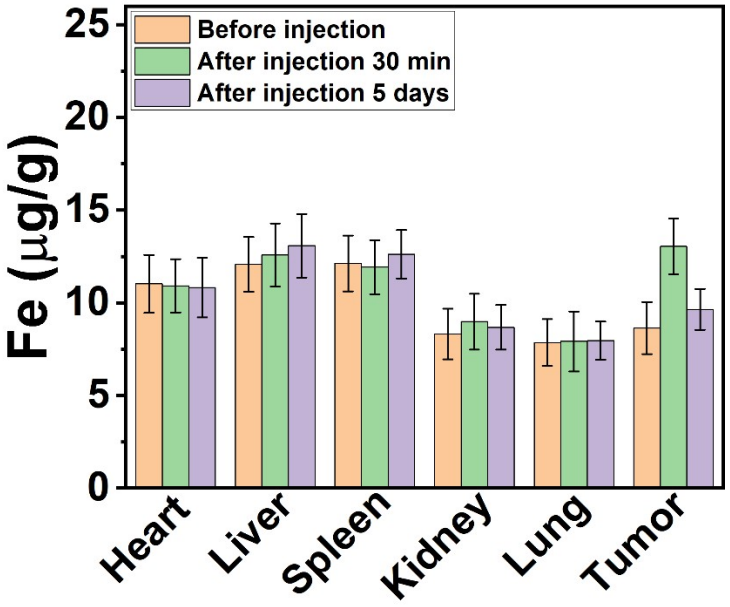

Fig. S22. Biodistribution of the levels of Fe element in major organs and tumors pre- and post-injection of CNPs@Fe.

Table S1. Comparison of the kinetic parameters of CNPs@Fe detected at pH 4.0 with other nanozymes.

Catalyst	Substrate	K_m (mM)	V_{max} (10^{-8} M s^{-1})	Reference
CNPs@Fe	TMB	0.303	11.7	This work
	H_2O_2	0.206	5.11	
$Cu_{2-x}Se$	TMB	0.532	2.05	1
	H_2O_2	0.457	0.38	
MoS_2–$Pt_{74}Ag_{26}$	TMB	25.71	7.29	2
	H_2O_2	0.386	3.22	
Fe_3O_4/N-GQDs	TMB	0.19	13.8	3
	H_2O_2	1.02	2.76	
MoS_2 (1100) NSs	TMB	2.6	6.7	4
	H_2O_2	0.016	8.3	
Cu-CN	TMB	0.26	1.98	5
	H_2O_2	3.00	2.59	
CuAsp	TMB	0.219 ± 0.009	4.138 ± 2.003	6
	H_2O_2	8.173 ± 0.756	2.291 ± 0.047	

1. H. Ni, X. Li, G. Yan, C. Huang and H. Zou, *Sensors and Actuators B: Chemical*, 2024, **398**, 134794.
2. S. Cai, Q. Han, C. Qi, Z. Lian, X. Jia, R. Yang and C. Wang, *Nanoscale*, 2016, **8**, 3685-3693.
3. B. Shi, Y. Su, L. Zhang, M. Huang, X. Li and S. Zhao, *Nanoscale*, 2016, **8**, 10814-10822.
4. C. Xia, L. Xu, Z. Li and L. Guo, *Applied Surface Science*, 2023, **635**, 157777.
5. J. Liu, X. Wang, F. Ma, X. Yang, Y. Liu, X. Zhang, S. Guo, Z. Wang, S. Yang and R. Zhao, *Chemical Engineering Journal*, 2022, **435**, 134966.
6. L. Lei, D. Song, L. Fan, B. Liu, M. He, X. Sun, W. Xu, K. Tao, H. Huang and Y. Li, *Microchimica Acta*, 2022, **189**, 61.

Table 2. The ratio of Fe^{2+}/Fe^{3+} in CNPs@Fe and Fe_3O_4.

CNPs@Fe	Relative Intensity Ratio (Fe^{3+}: Fe^{2+})	Fe_3O_4	Relative Intensity Ratio (Fe^{3+}: Fe^{2+})
Fresh	46.65% : 53.35%	Fresh	41.83% : 58.17%
pH 6.0	51.83% : 48.17%	pH 6.0	42.07% : 57.93%
pH 5.0	52.15% : 47.85%	pH 5.0	42.15% : 57.85%